

Modeling Blackout Dynamics in Power Transmission Networks with Simple Structure

B. A. Carreras
*Oak Ridge National
Laboratory*
Oak Ridge, TN 37831
carrerasba@ornl.gov

V. E. Lynch
*Oak Ridge National
Laboratory*
Oak Ridge, TN 37831
lynchve@ornl.gov

M. L. Sachtjen
*Oak Ridge National
Laboratory*
Oak Ridge, TN 37831

I. Dobson
*ECE Dept., University of Wisconsin
Madison, WI 53706 USA*
dobson@engr.wisc.edu

D. E. Newman
*Physics Dept., University of Alaska
Fairbanks, AK 99775 USA*
ffden@uaf.edu

Abstract

A model for blackouts in electric power transmission systems is implemented and studied in simple networks with a regular structure. The model describes load demand and network improvements evolving on a slow timescale as well as the fast dynamics of cascading overloads and outages. The model dynamics are demonstrated on the simple power system networks. The dynamics depend weakly on the network topologies tested. The probability distribution functions of measures of the cascading events show the existence of power-dependent tails.

1. Introduction

Electric power transmission systems are complex engineering systems with many interacting components. Their complete dynamical description involves detailed knowledge of each component and its coupling to the rest of the system. To model such a system, two approaches are possible. The most commonly used approach is a deterministic approach that models components in detail. Because all of the components and the physical laws that govern their interactions are known, it is possible to develop codes that describe particular blackouts. These codes may be complicated and time-consuming, but they are feasible. This approach has proven to be effective in helping to manage the power system. However, a different perspective can be taken. Blackouts in power systems happen quite frequently. These blackouts have a multiplicity of causes such as equipment failure, weather conditions, vandalism, and human error [1]. The dominant causes triggering blackouts cannot be written in the equations of a predictive code. Therefore, if we want to understand the global dynamics of power system blackouts, we

need to emphasize the random character of the events that trigger them and the overall response of the system to such events. This is the approach taken in this paper. The two approaches are necessary and complement each other. They may converge in the future when the second approach is further developed.

In following the second approach, it is sensible to start from a global, top-down perspective with simple models that capture the main effects only. However, there is a question to be faced: If the random events play a decisive role in triggering the system blackouts, how can we develop a simple model that is representative of the behavior of such a large and complex system? There is an answer to this question: If the system operates close to a "critical" point, some aspects of the response of the system to random perturbation may have a universal character. Therefore, we can hope to learn something from such modeling.

A recent analysis of blackouts in the North American power grid [2, 3] has shown that measures of such blackouts (such as megawatt hours unserved or number of customers affected) show the existence of long-range dependencies. Furthermore, the probability distribution function (PDF) of the size of the blackouts has a power law scaling. This behavior of the power transmission system is suggestive of a dynamical system close to a critical point. One possible governing principle for its dynamics is self-organized criticality [4].

We have considered a sequence of models that may reflect the dynamical properties of a self-organized critical system. The simplest model was employed in reference [3]. In [3] we used a sandpile model [5] as a black box to generate a

self-organized critical time series that could be compared to the time series of historical data for North American power grid blackouts. The sandpile was not a model for the dynamics of the power grid, but merely a means of testing the self-organized critical properties of the data.

The next step was taken by constructing a power transmission model [6] based on a cellular automaton similar to the sandpile model. This model allowed studying properties of network power transmission, but it did not solve the network power flow equations. The interesting result is that these two models produce PDFs of blackout sizes that are quite similar and are also similar to the PDF determined from the historical data for North American power grid blackouts.

Here we describe the implementation and results of a model [7] that takes it a step further by solving the network power flow equations. This model still remains simple, and in this paper we consider artificial power networks of homogeneous structure. In this way, we can vary a minimum number of parameters to explore the dynamics. However, extensions of the model are possible and easy to implement. These extensions will allow us to consider more realistic power system networks, incorporate the reliability of each component, and to vary the methods of responding to increasing power demand and improving the system.

2. Model Implementation

A model for the dynamics of power transmission networks was developed in [7]. We have implemented this model in a code written in C++. For each network, we define two types of classes, the node class and the line class. The node class represents the buses. They are either loads (L) or generators (G). (The node class can easily be generalized to combine both types of buses, but this has not yet been implemented.) Each node class contains the information on the type of bus, the instantaneous real power P_i (positive for generators and negative for loads), the maximum generator power P_i^{\max} , and to what other buses it is connected. The line class contains the information on the nodes i and j that the line connects, the instantaneous power flow F_{ij} , the maximum power flow F_{ij}^{\max} , and the line impedance z_{ij} . The present implementation allows only one line to connect two given nodes. This implementation of the model allows the consideration of any interconnected network

with $N_N = N_G + N_L$ nodes and N_I lines, where N_G is the number of generators and N_L is the number of loads. The present implementation does not allow the network to be disconnected and islanding cannot be studied.

As discussed in [7], the direct current (dc) power flow equations can be written in the form

$$F = AP, \quad (1)$$

where F is a vector whose N_I components are the line power flows F_{ij} , P is a vector whose N_N-1 components are the power injected at each node P_i , and A is a matrix that depends on the network structure and impedances. (The reference generator power P_0 is not included in the vector P to avoid the singularity of A as a consequence of the overall power balance.)

The dynamical evolution of the network involves two timescales. There is a slow timescale of days to years over which power demand changes and improvements to the system are made. There is also a fast timescale of minutes to hours over which a cascade of overloads and outages may take place. This cascade may lead to a blackout or back to normal operation. A flow diagram representing the overall operation of the code is shown in Fig. 1.

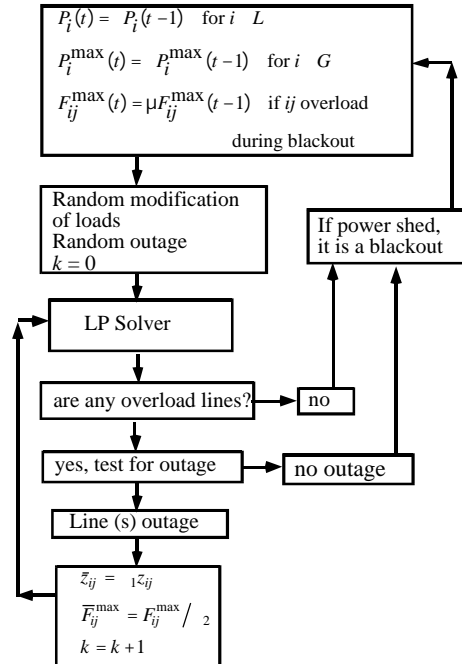


Fig. 1. Flow diagram of the implementation of the power transmission blackout model.

For simplicity, the daily peak load is chosen as representative of the loading during each day, and the events are computed based on that peak load. The timing of events in the cascade is neglected so that the cascade modeling moves through a possible sequence of states of the network rather than simulating the evolution of the cascade in time.

Slow timescale evolution

The dynamic of the long-term evolution of the network is carried out by a simple set of rules. At the beginning of day t , we apply the following rules:

1. Growth of the power demand. All loads are multiplied by a fixed parameter $\bar{\alpha}$, which is the average daily rate of increase in electricity demand. On the basis of the past rate of growth of electricity consumption, we estimated the parameter to be $\bar{\alpha} = 1.00005$. This value corresponds to a yearly growth rate of approximately 2%.

$$P_i(t) = \bar{\alpha} P_i(t-1) \quad \text{for } i \in L. \quad (2)$$

The maximum generator power is increased at the same rate:

$$P_i^{\max}(t) = \bar{\alpha} P_i^{\max}(t-1) \quad \text{for } i \in G. \quad (3)$$

2. Power transmission grid improvement. We assume a gradual improvement in the transmission capacity of the grid in response to the outages and blackouts. This improvement is implemented through an increase of the maximum line flow F_{ij}^{\max} for the lines that have overloaded during a blackout on the previous day (we will discuss the definition of a blackout later on in this section). That is,

$$F_{ij}^{\max}(t) = \mu F_{ij}^{\max}(t-1) \quad (4)$$

if line ij overloads during a blackout. We take μ to be a constant; μ is the main control parameter of the model.

3. Daily power fluctuations. To represent the daily fluctuations in power demand, all load powers are multiplied by a random number r , such that $1/r \leq r \leq 1$. We generally choose r in the range 1 to 1.4. We also assign a probability p_0 for a random outage of a line. We represent the line outage by multiplying the line

impedance by a large number α_1 and dividing the line maximum flow F_{ij}^{\max} by another large number α_2 . In the present calculations, α_1 and α_2 are of the order of 1000.

After applying these three rules to the network parameters, we solve the power flow problem using linear programming.

Linear programming solution of the power flow problem

Using the input power demand and grid parameters updated as indicated in the previous section, we solve the power flow equations (1) subject to constraints while minimizing the cost function:

$$\text{Cost} = \sum_{i \in G} P_i(t) - W \sum_{j \in L} P_j(t). \quad (5)$$

We assume that all generators run at the same cost and that all loads have the same priority to be served. However, we set up a high cost for load shed by setting $W = 100$. This minimization is done with the following constraints.

1. Generator power: $0 \leq P_i \leq P_i^{\max} \quad i \in G$
2. Load power: $P_j \geq 0 \quad j \in L$
3. Power flows: $|F_{ij}| \leq F_{ij}^{\max}$
4. Power balance: $\sum_{i \in G} P_i - \sum_{j \in L} P_j = 0$

This linear programming problem is numerically solved using the simplex method as implemented in [8].

In solving the time evolution problem, the initial conditions are chosen to be a feasible solution of the linear program (i.e., a solution satisfying the constraints). As the time evolution proceeds, we can reach a solution of the linear program that requires load shed or leads to overload of one or more lines. At this point, a cascade may be triggered, and the evolution moves to the fast timescale (Fig. 1).

Fast timescale evolution

Cascading overloads may start if one or more lines are overloaded in the solution of the linear program. We consider a line to be overloaded if the power flow through the line is within 1% of F_{ij}^{\max} . Each overloaded line is outaged with probability p_1 . Once one or more lines are outaged, the solution is recalculated.

This process can lead to multiple iterations and corresponds to the inner loop of the flow diagram in Fig. 1. The process goes on until a solution is found with no more outages. A blackout is defined as a cascading event in which the load shed is larger than a small value, typically 10^{-5} times the total power demand.

3. Dynamics of the slow timescale

We have considered several network structures, such as ring, tree, square, and hexagon networks. For the ring and tree networks, we have considered different numbers of couplings between the nodes. We have examined the sensitivity of the results to these different network structures. An example of a treelike network with three connections per node is shown in Fig. 2.

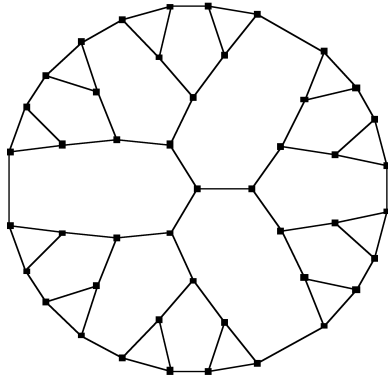


Fig. 2. Treelike 46 node network with 3 connections per node.

A reason to consider these networks is that their simple structure makes it easy to generate networks of different sizes. These networks have allowed us to carry out detailed scaling studies by varying the size and number of connections. Varying the size of the network allows the separation of scales needed to study finite size systems. The scaling studies are important in determining algebraic falloff of the PDFs of cascading events. For the numerical results presented in this paper, the network parameters are given in Table I.

Table I. Network parameters

Network	Number of nodes	Number of lines
Tree 46	46	69
Tree 94	94	141
Tree 190	190	285
Square 49	49	84
Hexagon 61	61	156

For these networks, we have arbitrarily assigned a generator at every tenth bus and loads at every other bus.

For a fixed rate of average increase of the power demand ($\bar{\mu} = 1.00005$), the effective power served depends on the rate of improvements μ in the grid. If the improvement rate is lower, there are more blackouts, and on average the power served is lower. We illustrate this effect in Fig. 3.

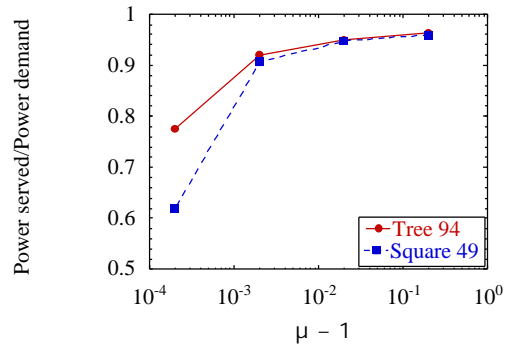


Fig. 3. Average ratio of the power served to the power demand as a function of the rate of improvement for two different network configurations.

Once the rate of improvement μ is given, there is a self-regulation process by which the system produces the number of blackouts that it needs to stimulate the response needed to meet demand. This is a necessary condition for the dynamical equilibrium of the system. The rate of increase in power demand for the overall system is essentially given by

$$R_D = (\bar{\mu} - 1)N_L.$$

(Note that $\ln \bar{\mu} \approx \bar{\mu} - 1$.) The system response is

$$R_R = (\mu - 1)f_{blackout} \langle \ell_o \rangle N_L,$$

where $f_{blackout}$ is the frequency of blackouts and $\langle \ell_o \rangle$ is a weighted average of lines overloaded in a blackout:

$$\langle \ell_o \rangle = \frac{F_{ij}^{max} \text{ (if line overloaded)}}{\text{lines} \cdot F_{ij}^{max}} \cdot \text{lines} \quad (6)$$

Dynamical equilibrium implies that $R_D = R_R$. This condition is well verified in all the numerical calculations, as shown in Fig. 4.

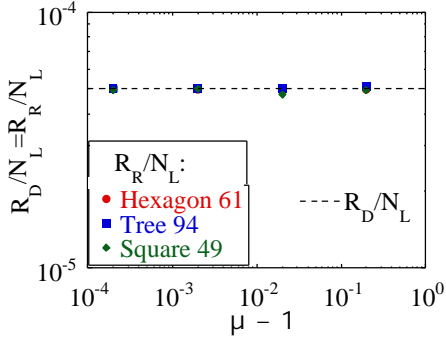


Fig. 4. Normalized rate of system response to the demand for three network configurations plotted as a function of μ . The response matches the demand (continuous line) in all cases.

The dynamical evolution reaches a steady state through a self-organization process as described in [7]. This process is well illustrated by the fractional overload

$$M_{ij} = \frac{F_{ij}}{F_{ij}^{max}}, \quad (7)$$

which measures how close each line works to its limit capacity. It is an observed property of the dynamical equilibrium that the time average of the fraction of overloads $\langle M_{ij} \rangle$ is independent of how the system is evolved to the dynamical equilibrium. The particular form of the distribution of $\langle M_{ij} \rangle$ over the lines depends on the structure of the network.

4. Dynamics of the fast timescale

In the present studies, we have assumed daily random fluctuations of the network loads with 1.2 1.4. The probability of a line outage when a line is overloaded is set to $p_1 = 0.3$. We have not yet explored the effect of varying p_1 . The other controlling parameter is p_0 , the probability of daily random line outages. We have kept p_0 at a value such that random line outages happen seldom (at average intervals of more than 30 days). Essentially, the results presented here are for the limit of very small values of p_0 for reasons that we will mention later.

The fast timescale dynamics are strongly coupled to the slow evolution. As discussed in the previous section, the improvements at rate μ are in response to the blackouts and outages. By fixing the improvement rate μ and the rate of growth of the demand μ , the system must have the number of blackouts needed to balance these two rates. Therefore, for a fixed rate of increase of the demand, it is not surprising that the frequency of blackouts is a strong function of μ . What is really interesting is that this blackout frequency does not depend much on the topology of the network. This is shown in Fig. 5.

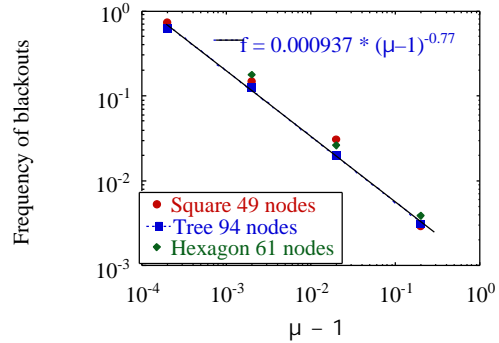


Fig. 5. Frequency of blackouts as a function of μ for three different networks. The straight line is a power fit.

The results in Fig. 5 can be summarized by a simple power dependence on $\mu-1$. The best fit to the results for all the networks in Table I gives an exponent -0.77 ± 0.01 . There is very little variation from one network to another. The coefficient of the power fit is somewhat more sensitive to the network characteristics.

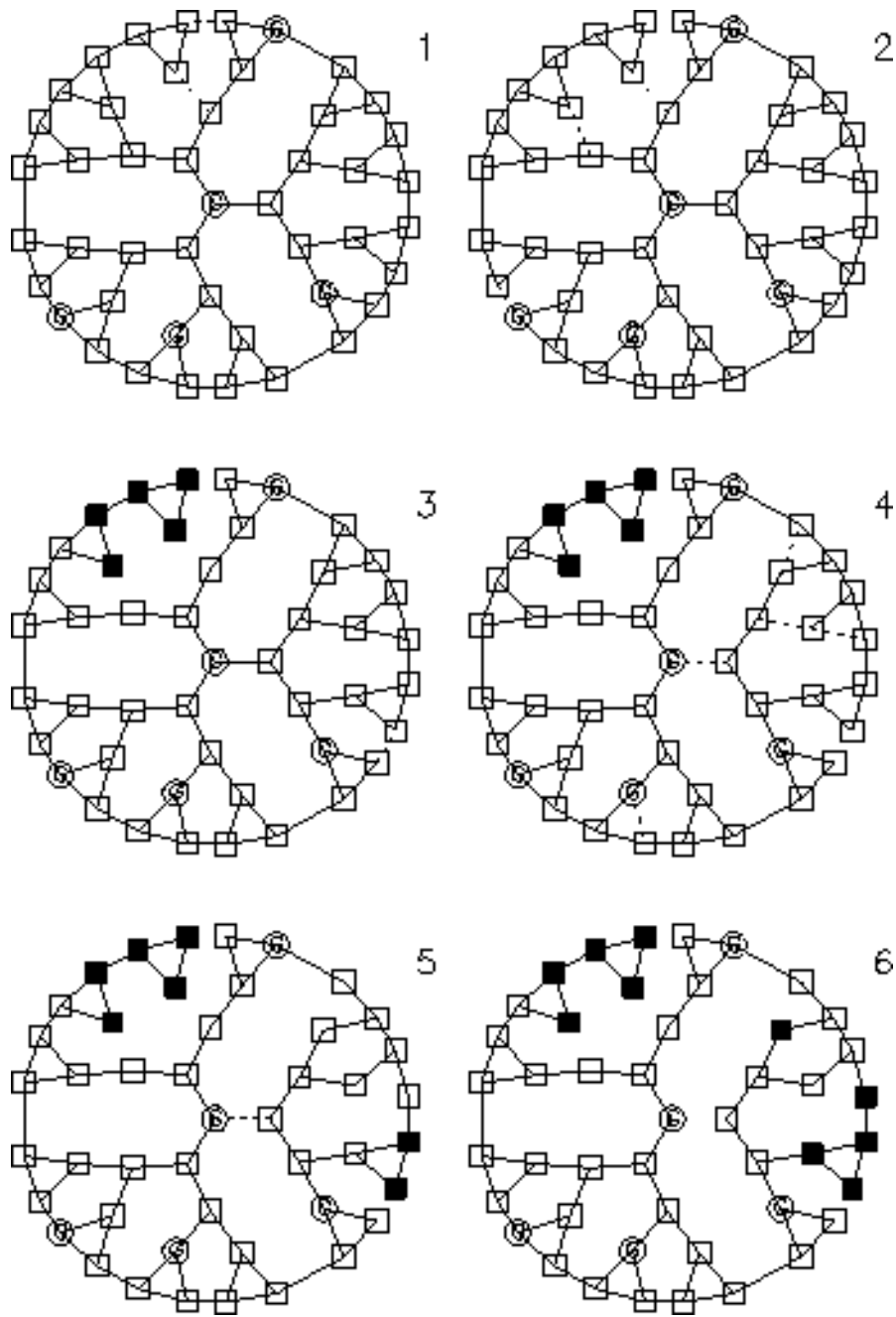


Fig. 6. Cascading events for the treelike network with 46 nodes that leads to a partial blackout of the network in 6 iterations.

The dynamics of the cascading events may involve several iterations during which lines are outaged and load is shed. As an example of such a process, we have plotted in Fig. 6 the status of the treelike 46-node network during a cascade. This particular cascade involves six iterations. Each of the six diagrams in the figure shows the status of the network after one of these iterations. The load nodes are represented by open squares, and the generator nodes are represented by open circles with the letter G inside the circle. The blackout nodes are depicted by black squares. At each iteration, the lines overloaded are plotted as broken lines, and the outaged lines are removed from the drawing. We have chosen this particular example because six iterations fit well into a page, but there are cascading events of all sizes as we will discuss later.

The cascade begins with a couple of line overloads in the upper region of the network. One of them causes an outage and triggers the process. The cascading process leads to a blackout of five buses in the upper region of the network graph. Simultaneously, a cascade is also triggered in the region of the network represented on the right hand part of the graph leading to five more loads blacking out.

The occurrences of cascading events are not correlated. Their triggers are random events. Therefore, the distribution of the waiting times between cascading events falls off with an exponential tail (Fig. 7).

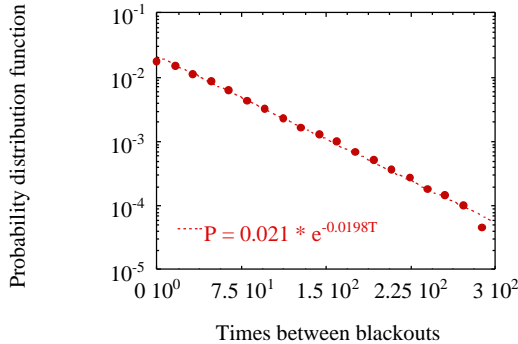


Fig. 7. Probability distribution function of waiting times between blackouts for the tree 96-node network with $\mu = 1.02$.

This decorrelation between triggering events is expected in a self-organized critical

model [9]. It has also been observed in an analysis of North American grid blackouts [3].

Although the PDF of the waiting times has an exponential falloff, the PDFs of the cascade sizes produced by the model have algebraic scaling regions. One measure of the cascade size is the total number of overloaded lines during the cascade. This measure has some parallelism with a measure of avalanche size in the sandpile model [5]. In Fig. 8, we have plotted the PDF of the overloads for three different networks and for $\mu = 1.002$.

There are several interesting points to note about Fig. 8. First of all, the three cases show very similar functional forms for the PDF. A second point is the existence of an algebraic region covering overloads between approximately 10 to 100. A fit in this region gives an exponent of -1.57. A third point is the faster falloff at larger number of overloads. This is probably due to the finite extent of the networks. Further calculations are needed with larger network sizes to test how the algebraic region scales with the size of the network.

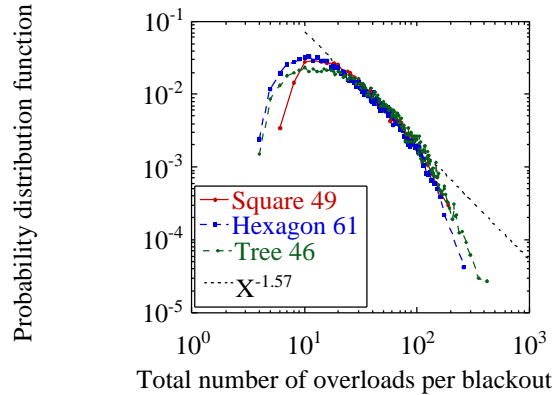


Fig. 8. PDF of the overloads for three different networks and for $\mu = 1.002$.

Although the size of the network clearly affects the sizes of the cascading events, it appears to have little impact on the frequency of the events. We have considered the three tree networks in Table I. They are characterized by tree connections at each node and they have 46, 94, and 190 nodes, respectively. For a fixed value of all input parameters, they seem to have the same frequency of blackouts (Fig. 9).

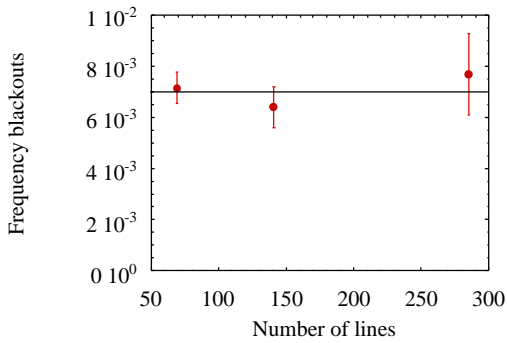


Fig. 9. Frequency of blackouts for the three tree networks listed in Table I.

The observed weak dependencies on the network structure are verified in the limit of p_0 very small and for a range of values of μ . As p_0 is increased, a different dynamical regime may set in. Strategies on how to respond to outages in this regime need to be developed and incorporated in the model. Because they have not been considered yet, we will not dwell on the characteristics of this operational regime. For large values of $\mu - 1$, such as an average daily rate of improvement of the grid higher than 3%, there is negligible dynamical activity, and very lengthy calculations are needed to have proper statistics. In contrast, if $\mu - 1$ is very small, below 0.01%, there are daily blackouts, and the model is no longer reasonable. In comparing the frequency of blackouts to the data for the North American grid [1], we find that a value of $\mu = 1.007$ is reasonable.

For a statistical analysis of the cascading events, we need to introduce some other measures of the size of the cascade. One possible measure is the amount of load shed during the cascading. However, since the overall power demand increases exponentially during the whole calculation, we normalize the load shed to the power delivered. In this way, we have a stationary sequence that can be analyzed with the usual statistical tools. The PDF of the load shed has an algebraic falloff and we can compare this PDF to the PDF of the avalanches of a sandpile as shown in Fig. 10. In Fig. 10, we have normalized the PDF of the avalanches to its maximum size. The results from the model are for a treelike 94-node network with $\mu = 1.002$. The sandpile has a length $L = 200$, which is of the same order as the number of lines in the network.

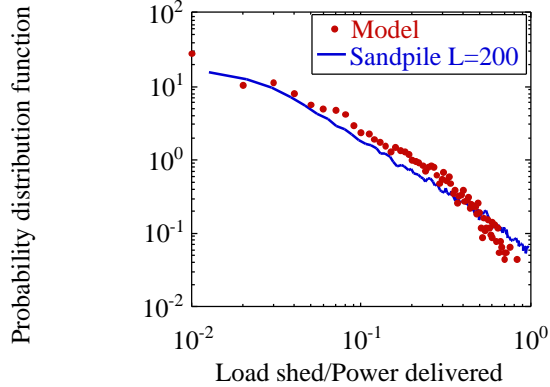


Fig. 10. PDF of the load shed divided by the power delivered compared to the PDF of the avalanches from a sandpile normalized to the maximum size.

As the parameter μ decreases, the frequency and the average size of the events increase. For small values of $\mu - 1$, we reach a situation in which the finite size of the system affects the size of the cascading event. We can see that through a sharp falloff of the PDF for large events. This finite size effect can distort the power dependence of the PDF (Fig. 11).

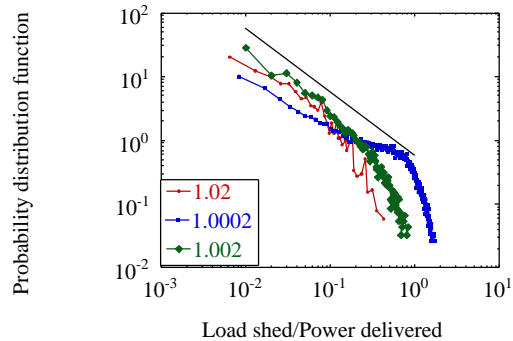


Fig. 11. PDF of the load shed divided by the power delivered for a square 49-node network.

5. Conclusions

We have presented the numerical implementation and some initial results of a dynamical model for blackouts in power transmission systems. The present implementation is minimal; that is, it uses

assumptions of uniformity of the components of the system, and all the control is by very few parameters. However, the model has the potential of incorporating inhomogeneities of the system and making the model more realistic.

In spite of the simplicity of the present model realization, the model shows very rich dynamics over both long and short timescales. The self-organization aspects of this model have been discussed elsewhere [7]. Here we have focused on the main properties of the cascading events.

The cascading events involve lines limiting, line outages, and possible load shed. When load shedding happens, we define the cascade as a blackout. Blackout frequency and size depend on the rate of improvement of the network μ . Thus, μ is the main control parameter in the present implementation of the model. The frequency and size of the blackouts depend weakly on the topology of the network, at least for the three topologies considered here. In addition, the distribution of the blackout sizes is a weak function of the topology. The distribution of blackout sizes has regions of power dependence falloff. The interpretation of these regions depends on the size of the network, and the present calculations have been limited to network sizes ranging from 69 to 159 lines. Larger network sizes are needed to better resolve these dependencies. However, the present calculations are consistent with possible self-organized critical behavior of the model.

6. Acknowledgements

Part of this research has been carried out at Oak Ridge National Laboratory, managed by UT-Battelle, LLC, for the U.S. Department of Energy under contract number DE-AC05-00OR22725. Ian Dobson and David Newman gratefully acknowledge support in part from NSF grants ECS-0085711 and ECS-0085647. Ian Dobson thanks H-D. Chiang and the School of Electrical Engineering at Cornell University for their generous hospitality during a sabbatical leave.

7. References

[1] Information on the electric system blackouts in North America was obtained from the North American Electric Reliability Council website at <http://www.nerc.com/dawg/database.html>.

[2] B. A. Carreras, D. E. Newman, I. Dobson, A. B. Poole, "Initial evidence for self-organized criticality in electric power blackouts," *Hawaii International Conference on System Sciences*, Maui, Hawaii, January 2000.

[3] B. A. Carreras, D. E. Newman, I. Dobson, A. B. Poole, "Evidence for self-organized criticality in electric power blackouts," *Hawaii International Conference on System Sciences*, Maui, Hawaii, January 2001.

[4] P. Bak, C. Tang, K. Wiesenfeld, "Self-Organized Criticality: An Explanation of 1/f Noise," *Phys. Rev. Letters*, vol. 59, pp. 381-384, 1987.

[5] T. Hwa, M. Kadar, "Avalanches, hydrodynamics, and discharge events in models of sandpiles," *Phys. Rev. A*, vol. 45, no. 10, pp. 7002-7023, May 1992.

[6] M. L. Sachtjen, B. A. Carreras, V. E. Lynch, "Disturbances in a Power Transmission System," *Phys. Rev. E*, vol. 61, no. 5, Part A, pp. 4877-4882, May 2000.

[7] I. Dobson, B. A. Carreras, V. E. Lynch, D. E. Newman, "An initial model for complex dynamics in electric power system blackouts," *Hawaii International Conference on System Sciences*, Maui, Hawaii, January 2001.

[8] W. H. Press, B. P. Flannery, S. A. Teukolsky, W. T. Vetterling, "*Numerical recipes in C*," Cambridge University Press, Cambridge, 1988.

[9] G. Boffetta, V. Carbone, P. Guliani, P. Veltri, A. Vulpiani, "Power laws in solar flares: self-organized criticality or turbulence?," *Phys. Rev. Letters*, vol. 83, pp. 4662-4665, 1999.